Effect of Addition of Ag and Cu on Strain Rate and Deformation Temperature on the Tensile Properties of Sn-5Sb Solder Alloy

M. Y. Salem[a,*], and A.S.Mahmoud[b]

[a] Physics Department, Faculty of Science at New Valley, Assuit University, 72511, El-Kharga, Egypt
[b]Physics Department, Faculty of Education, Ain Shams Univ., Cairo, Egypt
E-mail address: mahmoud_salem569@yahoo.com (M. Y. Salem)

About peritectic Sn-5Sb free solder alloy has encountered major attention for high temperature electronic applications, particularly on step soldering technology, flip-chip connection. In the running work, a small addition of quantity of Ag and Cu were combined to Sn-5Sb solder alloy to study the effect of a third element combination on the microstructural, thermal and mechanical properties. The study shows that the superplasticity of Sn-5Sb solder is reduced by Ag and Cu additions. The stress-strain curves gained were highly dependent on strain rate and temperature. More strain rates gave more stress-strain curve and more strain at fracture. The tensile manner of the alloys is strain rate and temperature dependence. Stress-strain characteristics of the Sn-5Sb binary, Sn-5Sb-1Ag and Sn-5Sb-1Cu ternary alloys were investigated at various strain rates (SR, $\dot{\varepsilon}$) from 5.56×10^{-4} to 1.26×10^{-3} s^{-1} and deformation temperatures from 303 to 403 K. Addition of 1Ag, and 1Cu to the binary Sn-5Sb alloy raised the yield stress σ_y, the ultimate tensile stress (UTS), and ductility (total elongation ε_T). Increasing the strain rate ($\dot{\varepsilon}$) increased both σ_y and (UTS) according to the power law $\sigma = C\dot{\varepsilon}^m$. A normal decrease of total elongation ε_T with strain rate ($\dot{\varepsilon}$) was observed according to an empirical equation of the form $\varepsilon_T = A\exp(-\lambda\dot{\varepsilon})$; A and λ are constants depending on the experimental condition. The results gained were explained in terms of the difference of the interior microstructure in samples. The Ag and Cu addition refines the microstructure, enhancing the mechanical properties, and form new intermetallic compounds (IMCs).

1. Introduction

Because the recognition of the hurtful effect of lead and lead including alloys on the environment and human health, many Pb-free solder-alloys have been advanced to substitute binary solders in electronic employment [1]. Near peritectic Sn-5Sb, Pb-free solder alloy has experienced great attention for elevation temperature electronic applications [2-4]; particularly on solder ball connections and bind a semiconductor device onto a substrate. It also has suggested as cathode materials for employ in Li ion batteries [5, 6]. The solder alloys is used to serve as a structural material to relate the components, the main

interest in the evolution of electronic packaging is the precision of the connects [7]. A applicable approximation to modify the accomplishment of a solder joint in terms of depressed melting point, more strength, perfect microstructure characteristic, and elevated creep resistance is to collect suitable another phase particles, or intermetallic, to a solder matrix [8,9].

Lead-free Sn-Sb solders have been particular as potential materials with elevated microstructure stabilization and perfect mechanical properties as approached to classical Pb-Sn solders [10–12]. The addition of solid barrier to dislocation movement can have heavy effects on the tensile strength and creep resistance of a metal. Deposition and dispersion encouragement have extradite important interest in the fields of high temperature structural materials owing to evident greater creep resistance. Mechanical and thermal property magnitude particular important excess in creep resistance, rupture time with the alloying of Ag and Cu.

For the precision of Sn-Sb, Pb-free solder alloy, Alam et al. [9] informed also that additions of Ag and Cu into the Sn-5Sb alloy can increase the solder characteristic, such as the ultimate tensile strength (UTS), and ductility, it is due to the construction of intermetallic compounds (IMCs) Cu_3Sn and Ag_3Sn. This can increase the microstructure stabilization and conserves the construction of SbSn precipitates in the solidification microstructure, thus significantly perfect their strength and ductility. For all samples, it was found that the UTS and yield stress (YS) raise with raising strain rate and decrease with raising temperature in tensile tests.

A Sn-5Pb (binary) solder is important for connecting electronic devices for printed circuit boards. Nowadays many electric and electronic units are mounted on automobiles. Different electric appliances used indoors, solder joints mounted on automobiles are used under more severe temperature conditions ranging from -30~176 ^{0}C for example. To ensure accuracy of these solder joints, the mechanical characteristics of solder under service properties should be recognized [13].

Binary solder samples are essential materials for combine electronic components on printed circuit boards due to their wonderful aggregation of material characteristic and a few cost. However, there are environmental and health danger related with the toxicity of lead present in the solder, and the possibility for small levels of Pb to deterioration the nervous system. The search for potential substitution alloys has covered an enormous area of comprehensive research in recent days.

The present work was completed to realize the effect of addition of Ag and Cu addition on the stress-strain characteristics of a binary solder alloy at various strain rates ranging from 5.56×10^{-4} to 1.26×10^{-3} s^{-1}, over a temperature range from 303 to 403 K.

2. Experimental Procedures

Sn-5Sb binary, Sn-5Sb-1Ag, and Sn-5Sb-1Cu ternary solder alloys were prepared from Sn, Sb, Ag and Cu (purity 99.99%) by vacuum melting. The ingots were rolled into wires. In this study, the wires were annealed at 413 K for 2 h and then slowly cooled to room temperature at a cooling rate T = $2x10^{-2}$ K/sec. After this heat treatment, the samples were annealed (left) at room temperature for 168 hour before testing. This process permitted a small amount of grain growth and grain stabilization to occur [14]. The microstructure of the samples was studied using X-ray diffraction and SEM. Stress strain deformation were performed on annealed wire samples of 0.4 mm radius and 5 cm standard length.

The samples were tested at temperature ranged from 303 to 403K under different strain rate ranging from $5.56x10^{-4}$ to $1.26x10^{-3}$ MPa, using a conventional type creep machine [6]. The accuracy of temperature measurement is of the order ± 1 K. Strain measurements were done with an accuracy of $\pm 1x10^{-5}$. The chemical compositions of the experimental alloys is represented in Table 1 and in Fig.(2); used Energy-dispersive X-ray spectroscopy (EDX) used in this investigation. A solution of 2% HCl, 3% HNO_3 and 95% (vol.%) ethyl alcohol was prepared and used to etch the samples.

Table (1): Actual compositions of the experimental alloys, wt.%.

Experimental alloys	Sn	Sb	Ag	Cu
Sn-5Sb	95	5	0	0
Sn-5Sb-1Ag	94	5	1	0
Sn-5Sb-1Cu	94	5	0	1

3. Results and Discussion

3.1. Microstructure change with addition of Ag and Cu

X-ray diffraction analysis was performed to determine the phase composition of the IMCs particles in the three as-cast Sn-5Sb, Sn–5Sb-1Ag and Sn-5Sb-1Cu alloys. As can be seen in Fig.(1), all the three as-cast alloys are mainly composed of peaks of precipitated SbSn phase. The Ag_3Sn phase was found in the XRD pattern of Sn-5Sb-1Ag alloy, indicating the successful alloying of Sn and Ag after the melting process. At the same time, the Cu_6Sn_5 phases were formed, which were due to the alloying of Sn and Cu in the Sn-5Sb-1Cu alloy. Moreover, the relative intensity of β-Sn was found to be slightly decreased with the addition of Cu, due to the formation of Cu_6Sn_5 phases. The microstructural development of the Sn–5Sb-based samples performs a necessary role in defining the mechanical properties of these samples.

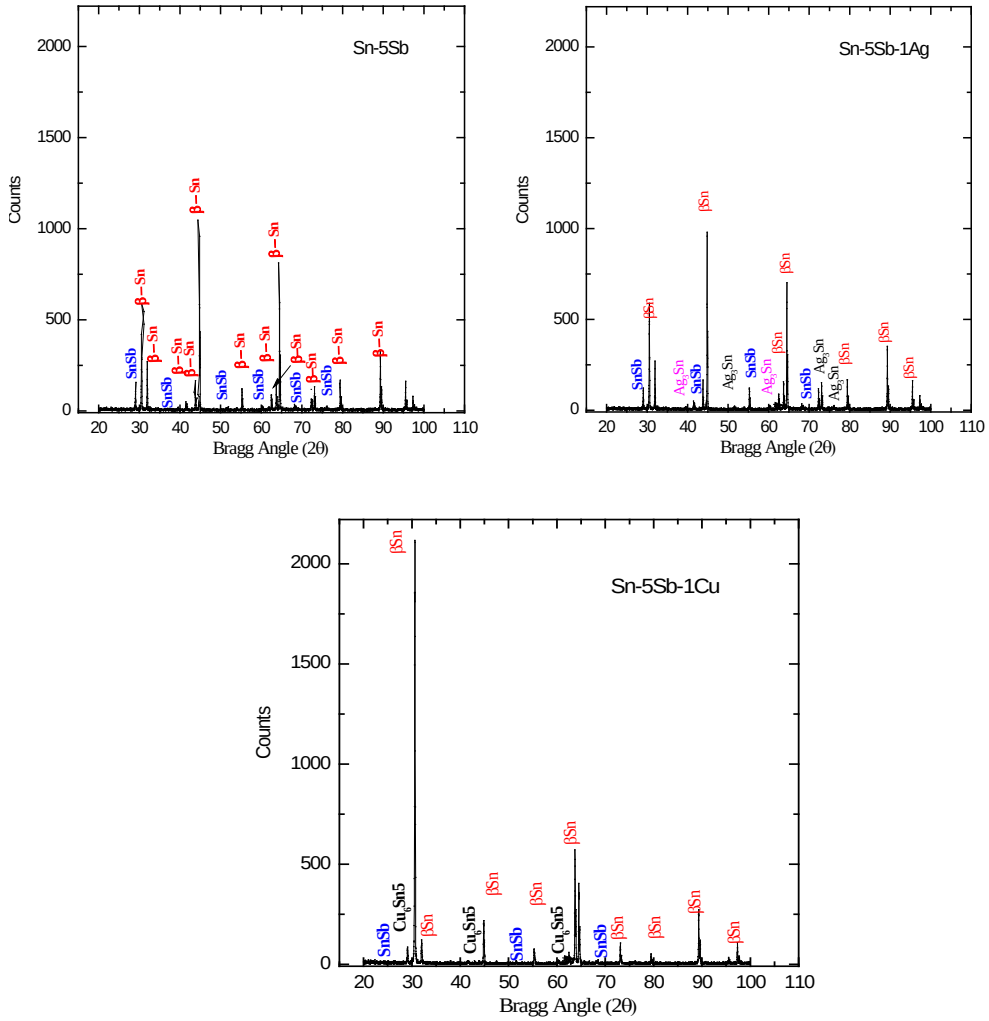

Fig. (1): XRD pattern for Sn-5Sb binary alloy are mainly composed of β-Sn phase and precipitated SnSb phase, (b) Sn-5Sb-1Ag ternary alloys containing of SnSb, β-Sn exhibited additional IMCs such as Ag_3Sn, and (c) Sn-5Sb-1Cu ternary alloys containing containing of SnSb, β-Sn exhibited additional IMCs such as Cu_6Sn_5.

Energy-dispersive X-ray spectroscopy (EDX), is an analytical technique used for the elemental analysis or chemical characterization of a sample. It relies on an interaction of some source of X-ray excitation and a sample. EDX pattern for the (Sn-5Sb, Sn-5Sb-1Ag and Sn-5Sb-1Cu alloys) alloy is shown in Fig.(2). Using EDX analysis, the percentage of Sn, Sb , Ag, and Cu are found similar to that value in Table (1)

Figure (3): The SEM images of the alloys are presented in Fig.(3a) Sn-5Sb, alloys microstructure composed of light gray areas of Sb and dark network-like eutectic regions of β-Sn grain boundaries. In Fig.(3b), the appropriate content of Ag in the Sn-5Sb solder was found to improve the microstructure of the alloy, there is Ag3Sn IMCs., In Fig.(3c), the Cu6Sn5 IMCs might act as heterogeneous nucleation sites for β-Sn dendrites upon solidification and are able to refine the grain size of Sn-5Sb alloy. Consequently, the mechanical properties of Sn-5Sb-1Cu solder may be enhanced.

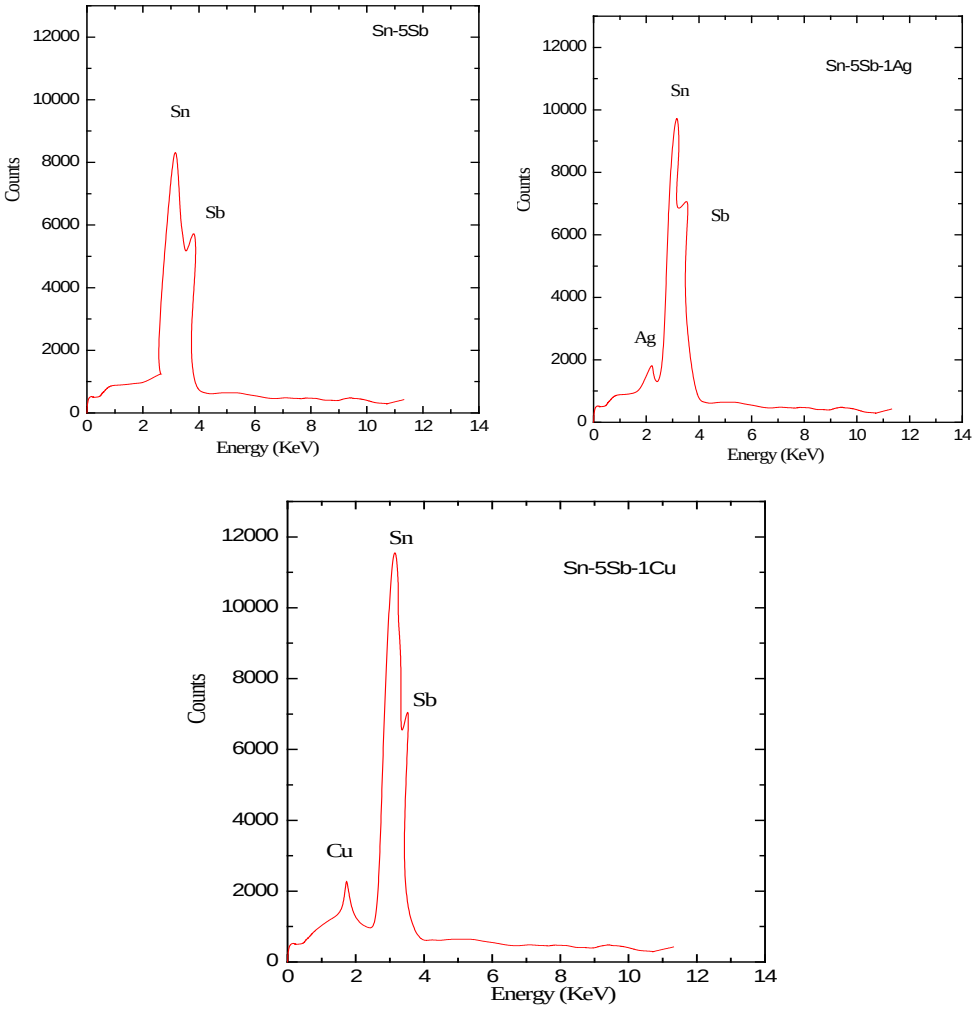

Fig.(2): Energy-dispersive X-ray spectroscopy pattern for Sn-5Sb, Sn-5Sb-1Ag and Sn-5Sb-1Cu.

Fig.(3): The SEM images of the alloys are presented in Fig.(18a) Sn-5Sb, alloys microstructure composed of light gray areas of Sb and dark network-like eutectic regions of β-Sn grain boundaries, X=2000 In Fig.(18b), the appropriate content of Ag in the Sn-5Sb solder was found to improve the microstructure of the alloy, there is Ag_3Sn IMCs X=1000., In Fig.(18c), the Cu_6Sn_5 IMCs might act as heterogeneous nucleation sites for β-Sn dendrites upon solidification and are able to refine the grain size of Sn-5Sb alloy. Consequently, the mechanical properties of Sn-5Sb-1Cu solder may be enhanced X=1000.

3.2. Tensile properties

The effect of Ag and Cu additions on the mechanical properties of binary solder at 303K can be seen from stress-strain curves as shown in Fig. (4), Fig.(5) represented the relation of stress-strain curves at 323 K, Also stress-strain for 343 K, and 363 K are shown in Figs.(6,7). it is shown that Sn-5Sb-1Cu is more strengthening than Sn-5Sb-1Ag and also binary.

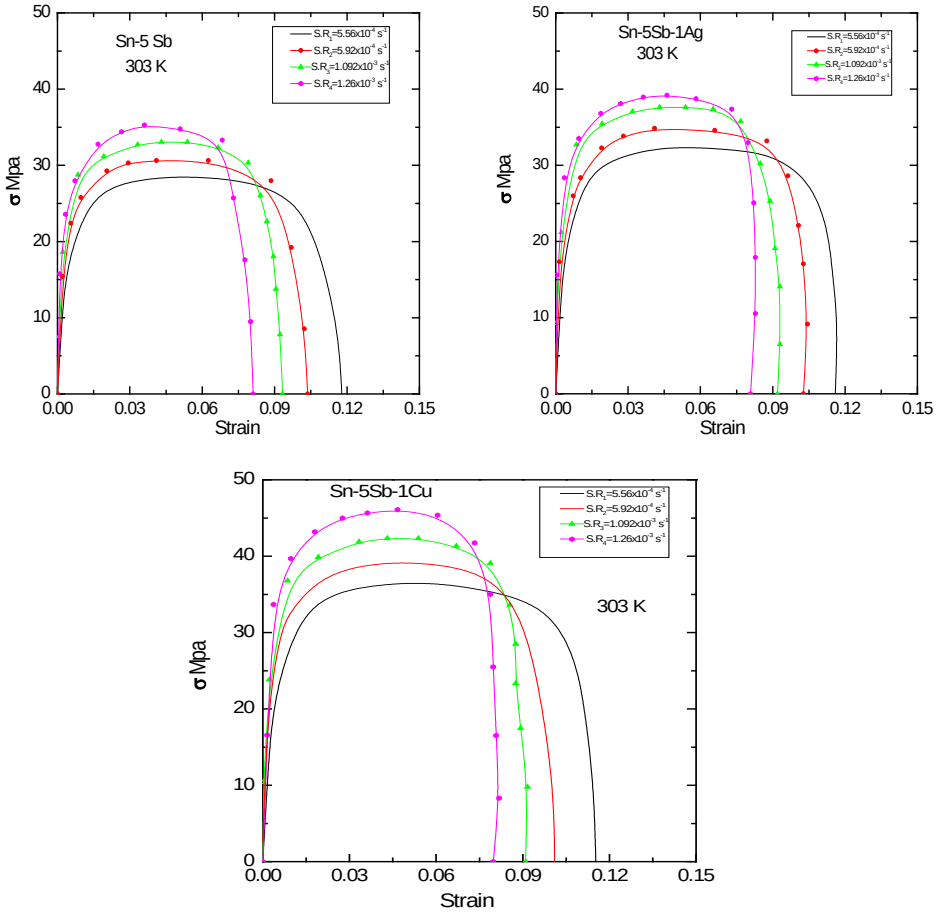

Fig.(4): Comparative tensile stress-strain curves obtained at 303K and different strain rate for Sn-5Sb, Sn-5Sb-1Ag and Sn-5Sb-1Cu solder alloys.

The effect of Ag and Cu additions on the stress-strain curves of Sn-5Sb binary alloys at different temperature and constant strain rate equal $5.56x10^{-4}$ s^{-1} is shown in Fig.(8)., UTS values of Sn-5Sb, Sn-5Sb-1Ag, and Sn-5Sb-1Cu decreased with increasing temperature. Fig. (9) list the variation of Young's modulus (Y) with strain rate at different working temperature for Sn-5Sb, Sn-5Sb-1Ag and Sn-5Sb-1Cu. The Variation of yield stress (σ_y) with strain rate at different working temperature for Sn-5Sb, Sn-5Sb-1Ag and Sn-5Sb-1Cu is shown

in Fig.(10). The relation between the fracture strength (breaking strength) σ_f and strain rate at different working temperature for Sn-5Sb, Sn-5Sb-1Ag and Sn-5Sb-1Cu is illustrated in Fig. (11).

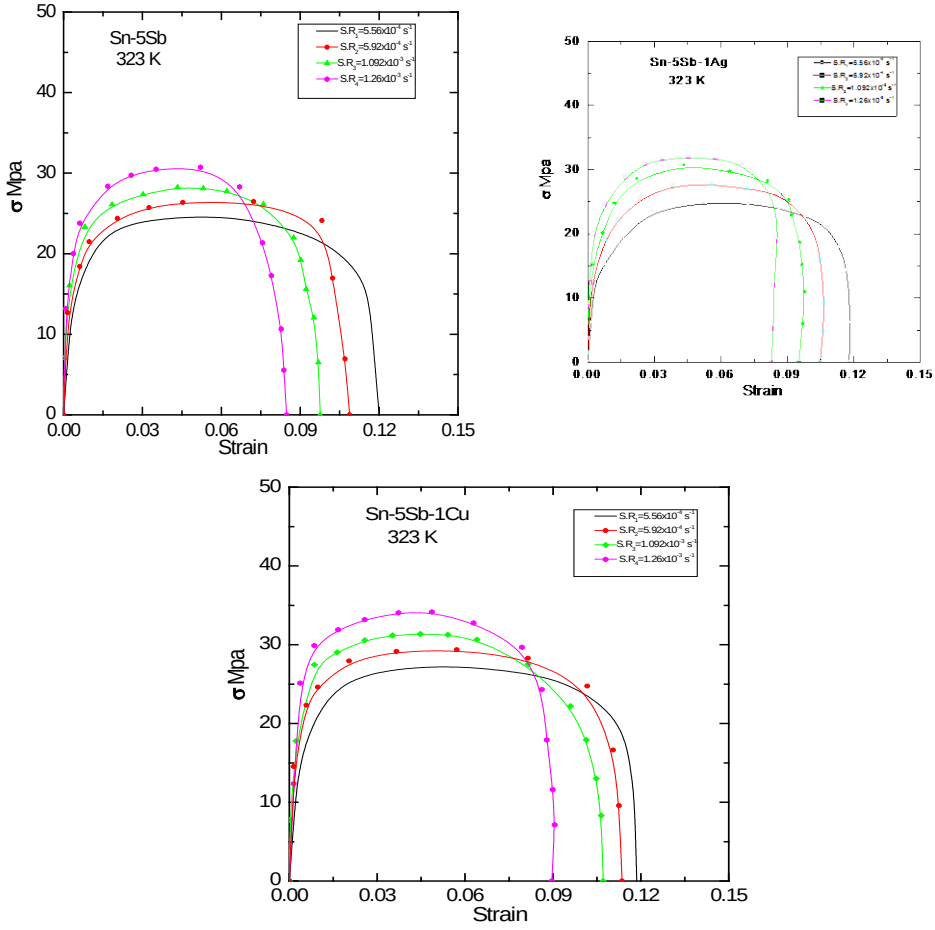

Fig.(5): Comparative tensile stress-strain curves obtained at 323K and different strain rate for Sn-5Sb, Sn-5Sb-1Ag and Sn-5Sb-1Cu solder alloys.

The strain rate dependence of the total elongation ε_T It was found to obey an empirical relation of the form:

$$\varepsilon_t = A \exp(-\lambda \dot{\varepsilon}) \qquad (1)$$

where A and λ are constants depending on the tensile test conditions. From the Fig. (4-8), it is obvious that the total elongation in alloys reducing with rising strain rate. However, in the Ag, and Cu free alloy, the values of ε_T are lower with increasing temperature at all strain rates Fig.(4-8). While in the Ag, and Cu containing alloy the values of ε_T increase with temperature at all strain rates. This variation in the relation between tensile elongation as a function of strain rate and temperature seems to depend on the variation in the microstructure of the alloys.

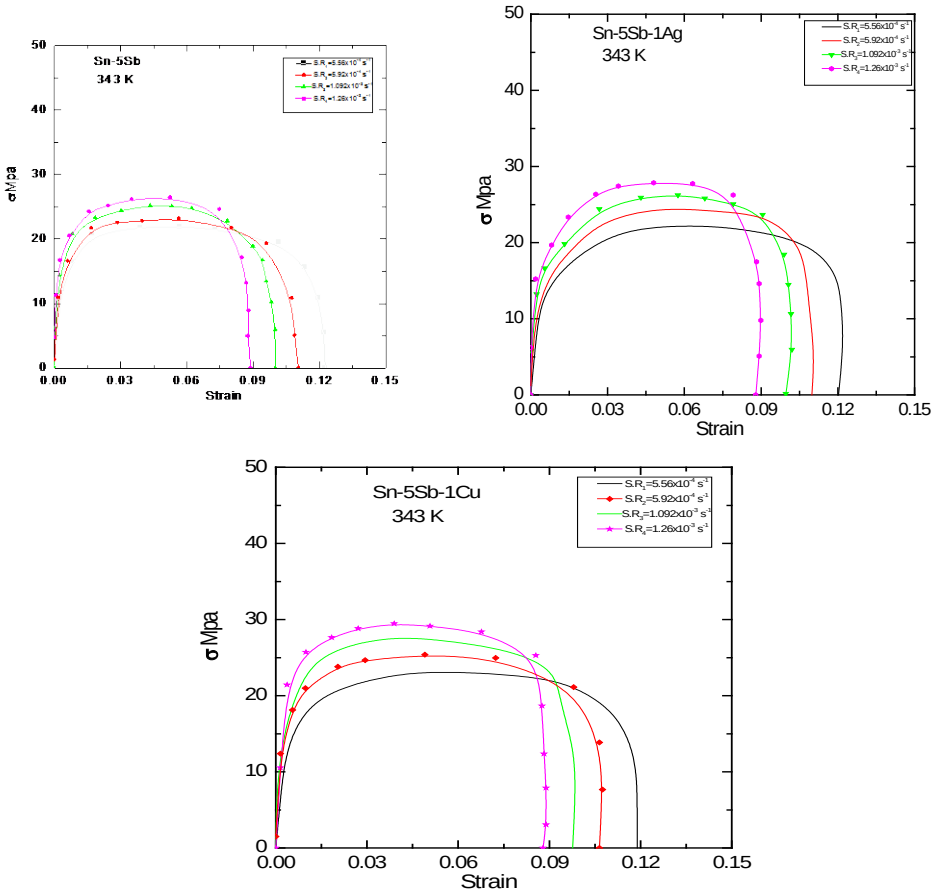

Fig.(6): Comparative tensile stress-strain curves obtained at 343K and different strain rate for Sn-5Sb, Sn-5Sb-1Ag and Sn-5Sb-1Cu solder alloys.

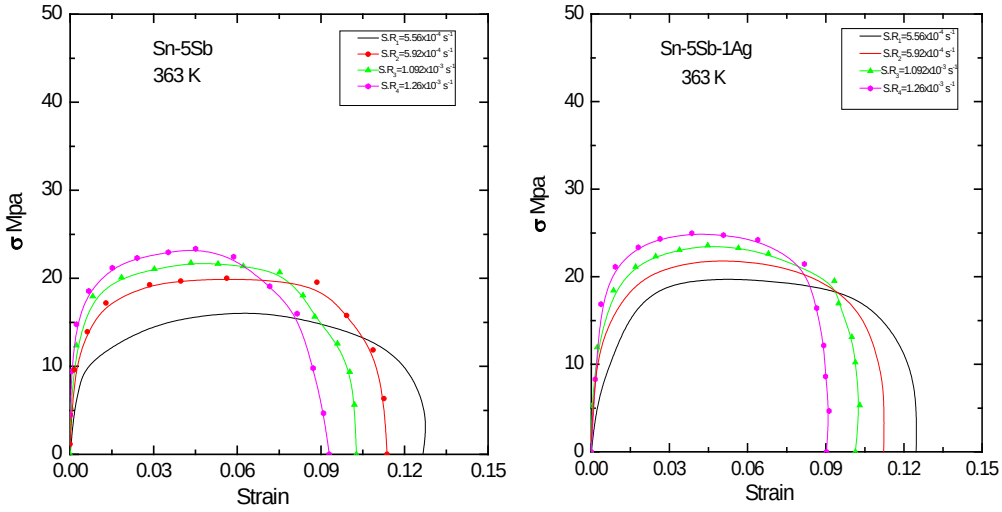

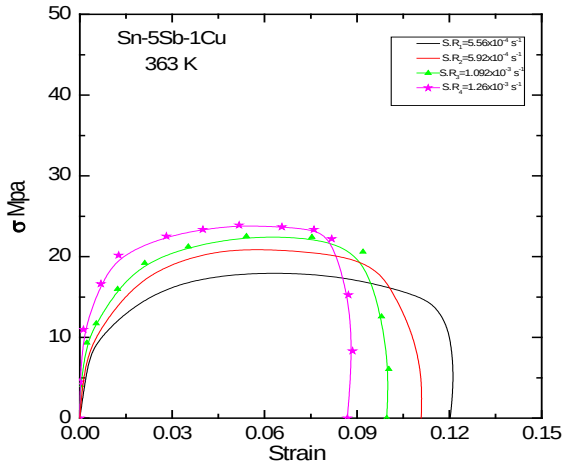

Fig.(7): Comparative tensile stress-strain curves obtained at 363K and different strain rate for Sn-5Sb, Sn-5Sb-1Ag and Sn-5Sb-1Cu solder alloys.

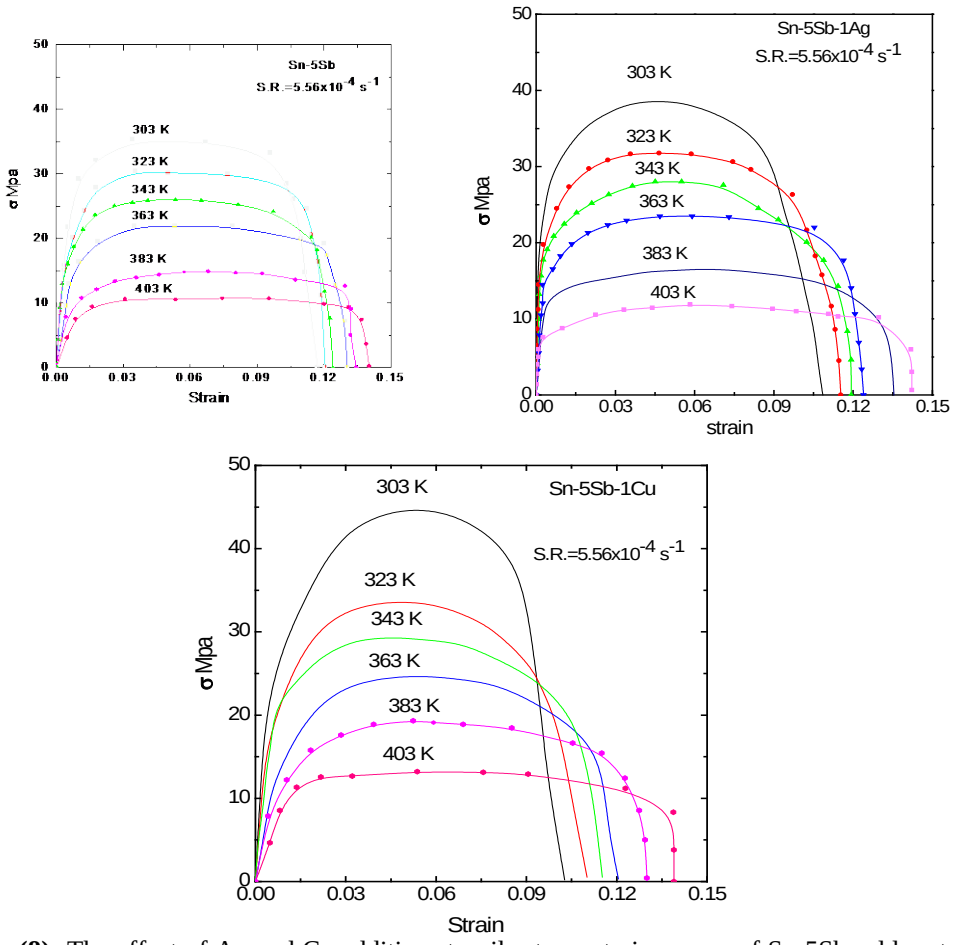

Fig.(8): The effect of Ag and Cu additions tensile stress-strain curves of Sn-5Sb solder at different temperature and constant strain rate $5.56x10^{-4}$ s^{-1}.

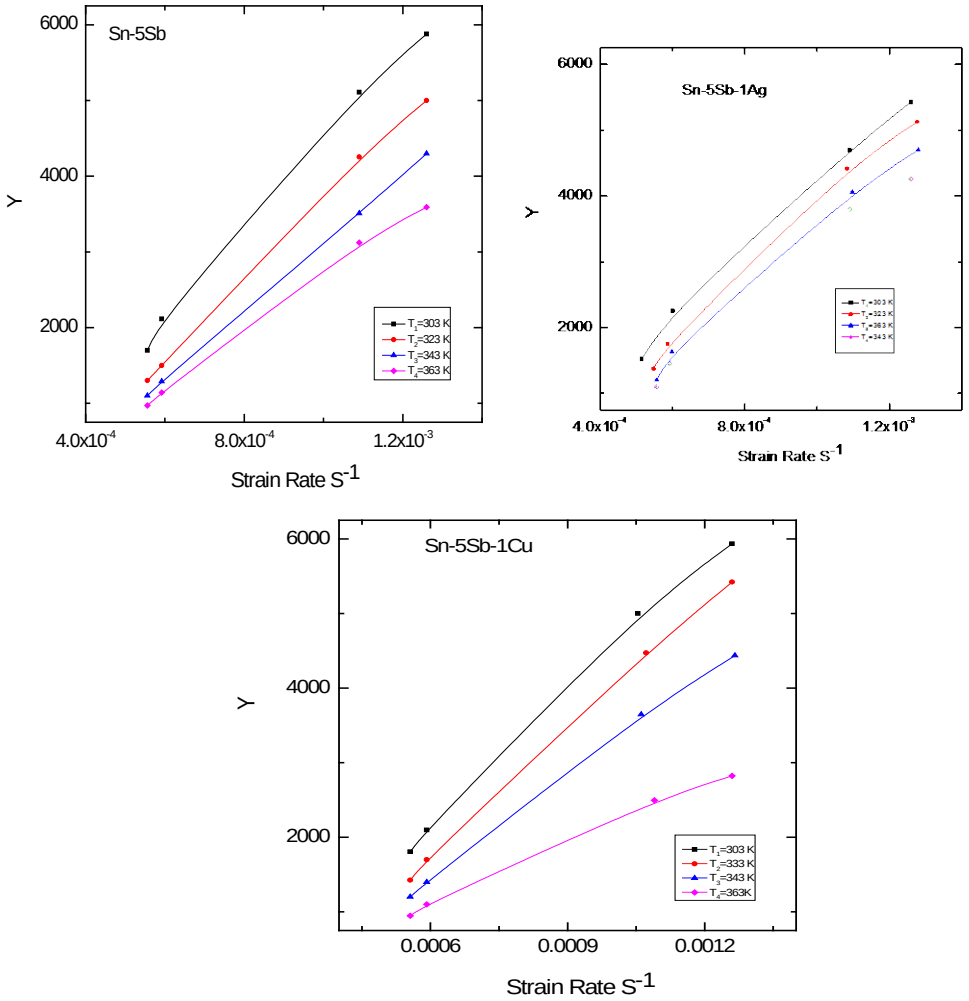

Fig.(9): The comparison of Young's modulus (Y) with strain rate at different working temperature for Sn-5Sb, Sn-5Sb-1Ag and Sn-5Sb-1Cu

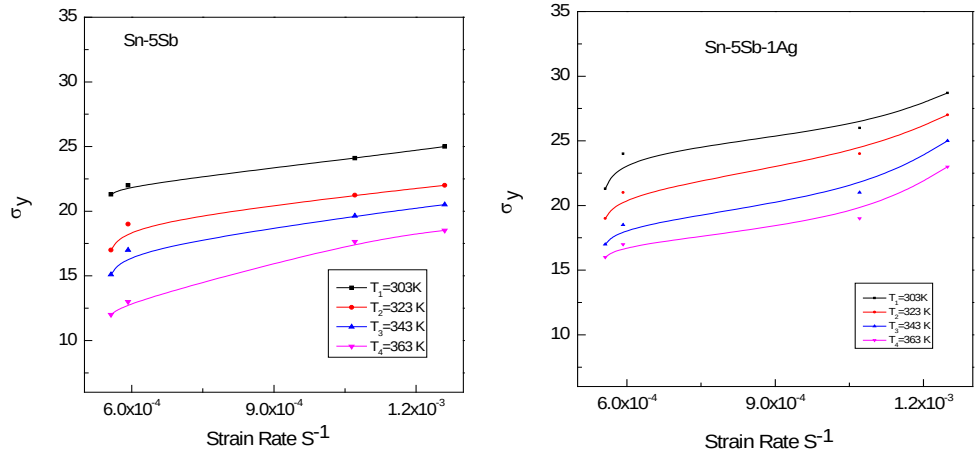

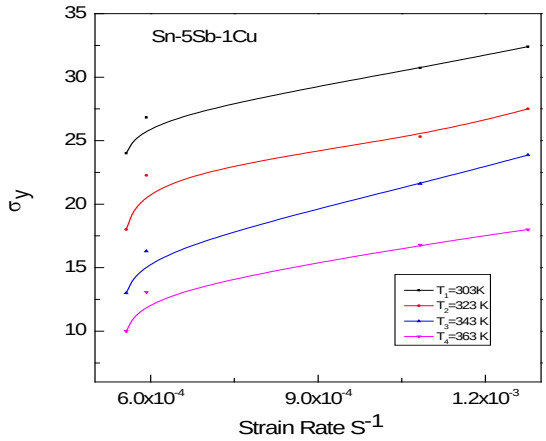

Fig.(10): The Variation of yield strength (σ_y) with strain rate at different working temperature for Sn-5Sb, Sn-5Sb-1Ag and Sn-5Sb-1Cu.

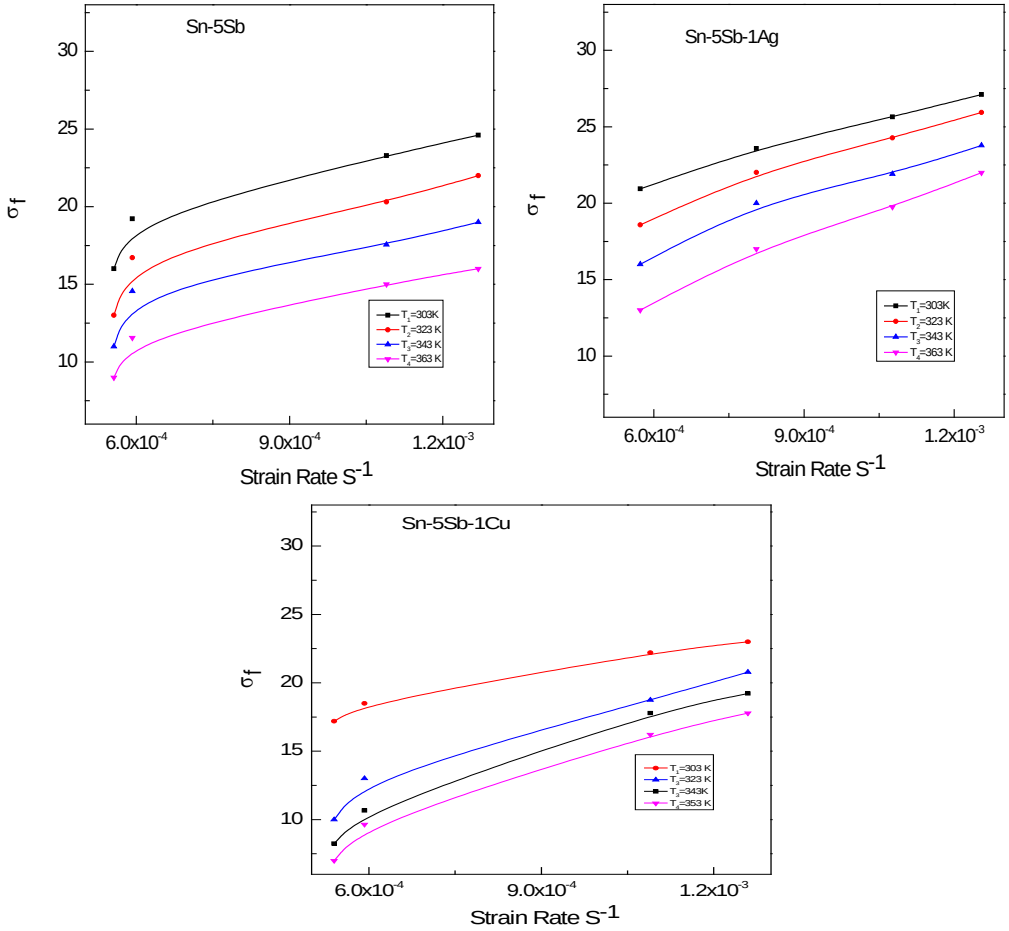

Fig.(11): illustrated the fracture strength (σ_f) with strain rate at different working temperature for Sn-5Sb, Sn-5Sb-1Ag and Sn-5Sb-1Cu.

It is noted that the stress strain parameters, the yield stress, fracture strength, and the total elongation of all alloys are highly influenced by the difference of the strain rate and deformation temperature.

3.3. Strain rate and temperature dependence of the ultimate tensile stress (UTS)

The variation of the ultimate tensile stress (UTS) with strain rate at different working temperature for Sn-5Sb, Sn-5Sb-1Cu and Sn-5Sb-1Ag is illustrated in Fig. (12).

It is shown that the relation between the strain rate (SR) and the ultimate tensile stress (UTS) for the alloys at different deformation temperatures, increasing SR ($\dot{\varepsilon}$) increases the UTS in three alloys. This is because of increasing strain rate is accompanied by an increase in the dislocation density. As these dislocations move they become tangled. It is then more difficult for other dislocations to glide through the material, especially at the lower deformation temperatures. Note that the Ag, and Cu containing solder alloy samples exhibited higher UTS than those exhibited by the binary Sn-5Sb at all deformation temperatures. The higher values of the UTS in the alloy may be attributed to the refinement and uniform distribution of the intermetallic Ag_3Sn, and Cu_6Sn_5 particles, it seem to provide a greater measure of dispersion strengthening due to the finer particle size in the ternary alloy compared to the binary alloy.

The UTS values of Sn-5Sb, Sn-5Sb-1Ag, and Sn-5Sb-1Cu were 35.4, 39.1 and 45.64MPa, respectively. The Sn-5Sb alloy had the lowest UTS and elongation, while Sn-5Sb-1Ag had intermediate values, and the Sn-5Sb-1Cu alloy had both the highest UTS and elongation. Increasing the UTS of Sn-5Sb-1Cu alloy is due to softest nature of this alloy.

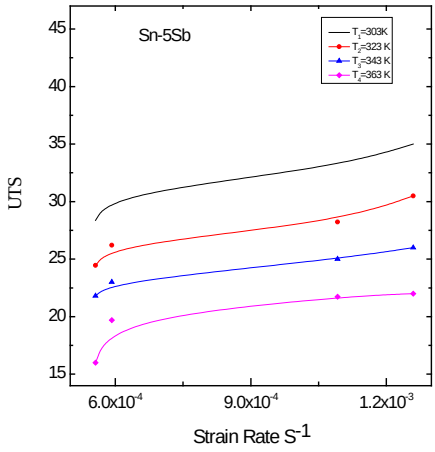

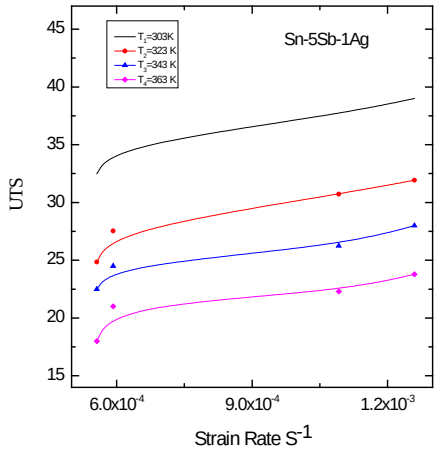

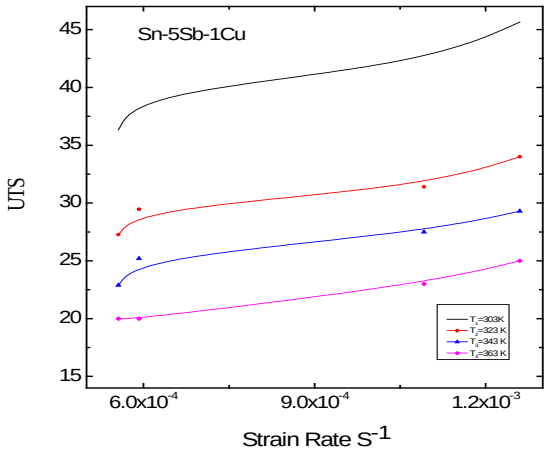

Fig.(12): The variation of the ultimate tensile stress (UTS) with strain rate at different working temperature for Sn-5Sb, Sn-5Sb-1Ag and Sn-5Sb-1Cu.

For the three alloys at the same deformation temperature, increasing the strain rate gives rise to higher values of yield strength, fracture strength, and UTS as seen in Fig.(4-8), and decrease in fracture strain as seen in Fig.(13).

At the same strain rate, raising the deformation temperature results in a continuous softening; a decrease in yield strength, fracture strength, and UTS was observed. From this figure, at constant strain rate a increase of working temperature results in increase in fracture strain as seen in Fig.(13).

It is also interesting to note that the increased ductility of ternary alloy is completed without sacrificing the mechanistic intensity. However, after the stress levels rise up to yield strength of the solder alloys, the strain hardening, instead of strain softening, has occurred in all the as-solidified solder alloys, which may enhance the ultimate tensile stress and yield strength in these samples [15].

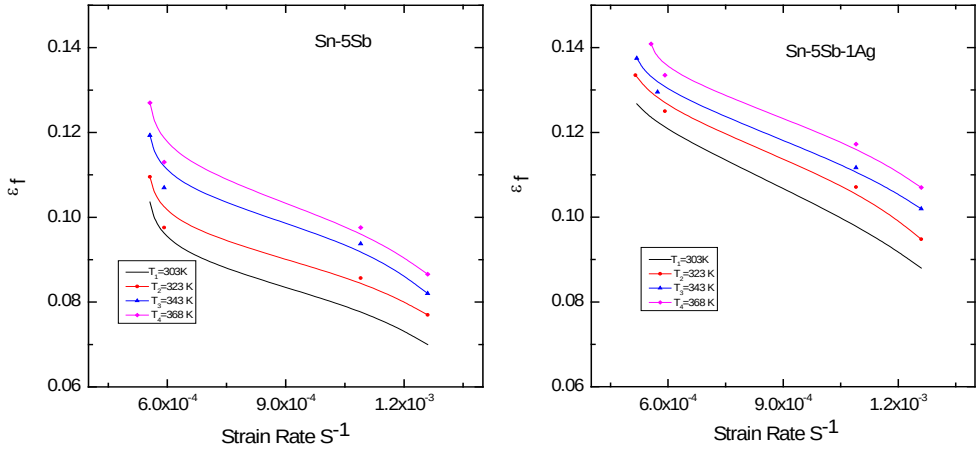

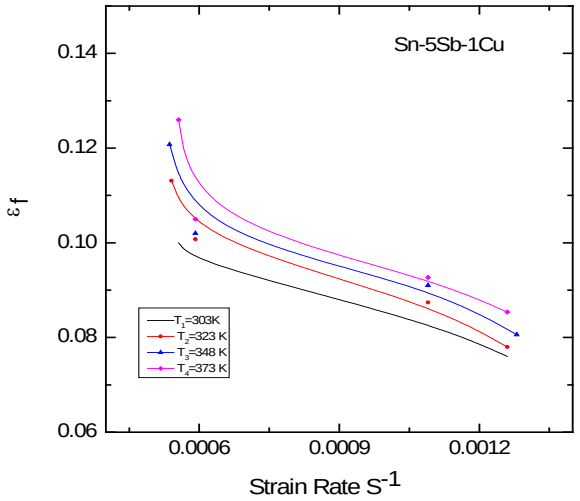

Fig.(13): The variation of the fracture strain (ε_f) with strain rate at different working temperature for Sn-5Sb, Sn-5Sb-1Ag and Sn-5Sb-1Cu.

Since the distortion resistance of samples was defined crucial important mechanical property, a good deformation resistance suggests great plastic region. Compared with the Sn-5Sb alloy and Sn-5Sb-1Cu alloy solders, which have a little deformation resistance, an excellent deformation resistance and long plastic region of Sn-5Sb-1Ag alloy would insure this solder to become one of prefer for replacing the Sn-5Sb solder in microelectronic packaging and interconnecting. The addition of 1Ag was adequate to stimulate a great change in the mechanical properties. This point out that the immovability to necking has been modified because of the high interface formed between SbSn and Cu_6Sn_5 IMCs with the β-Sn matrix, which in turn enhanced both ultimate tensile stresses [15]. While, the Ag_3Sn IMCs particles formed in the Sn-5Sb-1Ag alloy can strongly enhance the ultimate tensile stress UTS of this alloy because of lower elastic modulus of these IMCs inside the solder matrix. These results are consistent with the previous finding [16] that the Cu_6Sn_5 often exhibits a larger elastic modulus than Ag_3Sn IMCs when alloying 1.5Ag and 0.7Cu to Sn–9Zn solder, respectively.

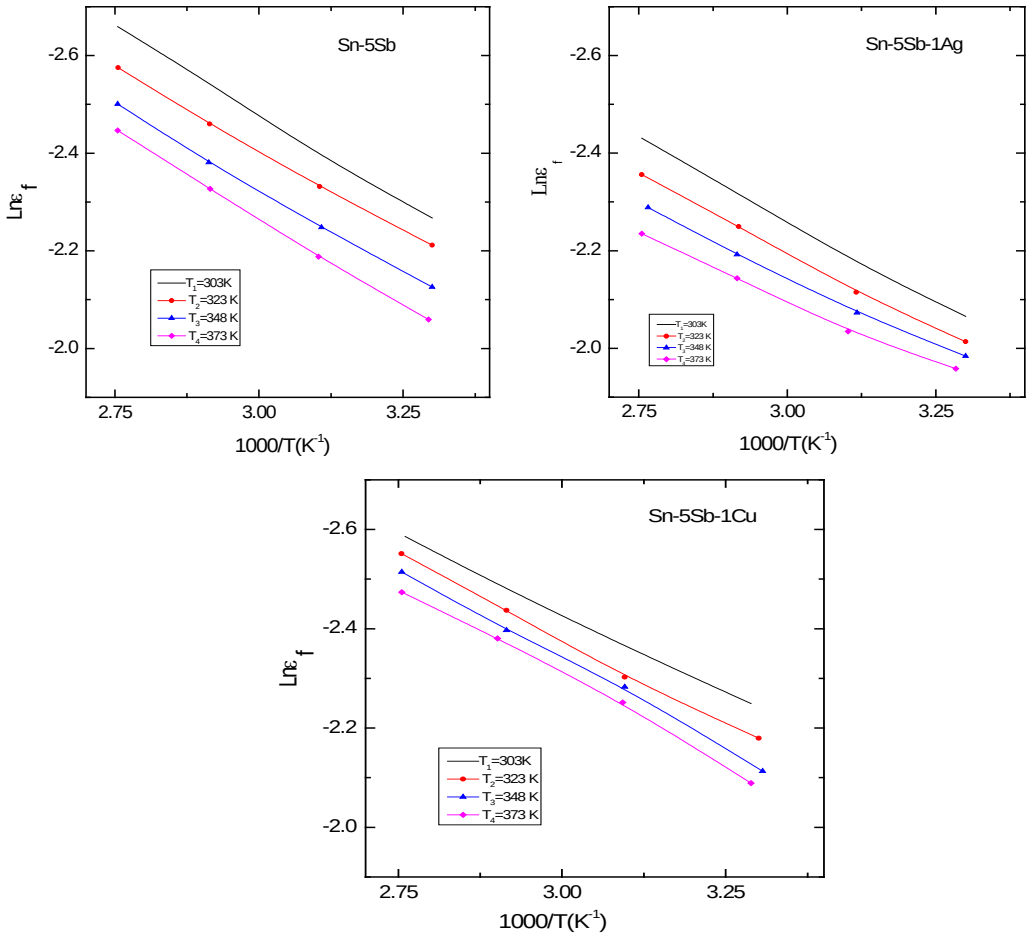

Fig.(14): The relation between ln fracture strain (ε_f) with 1000/T at different working temperature for Sn-5Sb, Sn-5Sb-1Cu and Sn-5Sb-1Ag.

3.3. Stress exponents and activation energy

Tensile deformation mechanisms are identified by the values of n and the activation energy Q. In fact, deformation of polycrystalline materials at temperatures above 0.5 T_m can take place by different deformation mechanisms, associated with different stress exponent values. Diffusional creep is associated with n values around 1. The relationship of stress–strain of Sn-based solder alloys is usually expressed by the power-law of the type [17].

$$\dot{\varepsilon} = A\,\sigma^n \exp(-Q/RT) \qquad (2)$$

The activation energy can be calculated from the relation between ln fracture strain (ε_f) with 1000/T at different working temperature for Sn-5Sb, Sn-5Sb-1Ag and Sn-5Sb-1Cu as seen in Fig.(14). The value of activation energy

with strain rate for Sn-5Sb, Sn-5Sb-1Ag and Sn-5Sb-1Cu seen in Fig.(15a). The relation between lnε̇ And ln σ for all samples are shown in Fig.(15b), the value of n stress exponent is determined from the slope of this Fig, the value on n is around 0.87 : 0.9 .

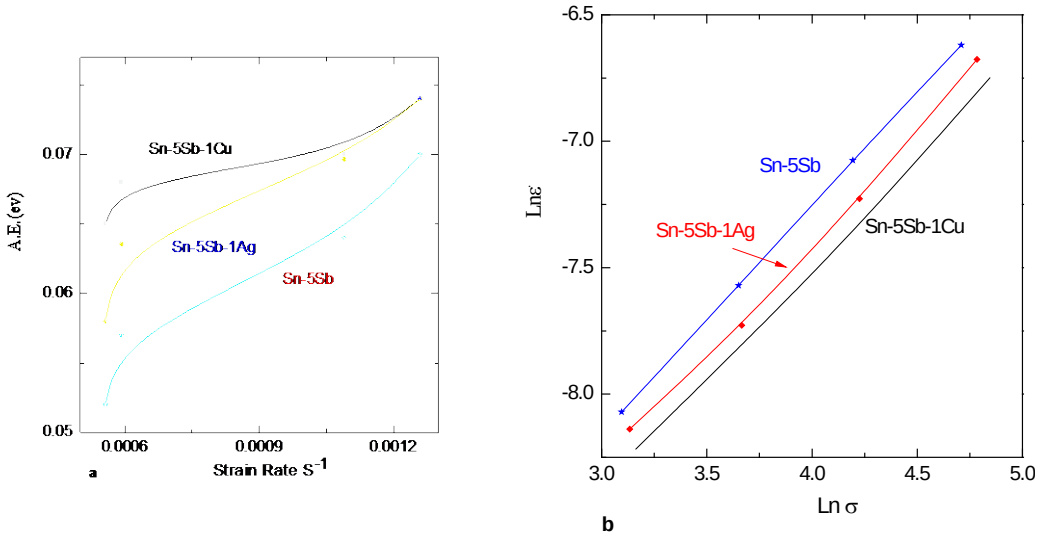

Fig.(15): a; The activation energy with strain rate for Sn-5Sb, Sn-5Sb-1Ag and Sn-5Sb-1Cu. b); illustrated lnε̇ lnσ at different working temperature for Sn-5Sb, Sn-5Sb-1Cu and Sn-5Sb-1Ag.

4. Conclusion

1. For all alloys, YS increased with increasing strain rate and decreased with increasing temperature, and appears to be a sensitive parameter of morphology and processing parameters of the alloys whereas the ductility changes were generally large for the ternary Sn-5Sb-1Cu alloy.
2. The UTS values of Sn-5Sb, Sn-5Sb-1Ag, and Sn-5Sb-1Cu increased with increasing strain rate and decreased with increasing temperature were 35.4, 39.1 and 45.64MPa, respectively. The Sn-5Sb alloy had the lowest UTS and elongation, while Sn-5Sb-1Ag had intermediate values, and the Sn-5Sb-1Cu alloy had both the highest UTS and elongation. Increasing the UTS of Sn-5Sb-1Cu alloy is due to softest nature of this alloy.
3. The formation of fine β-Sn grain size and distribution of fine needle-like Cu–Sn IMC phases in the Sn-5Sb-1Cu solder matrix were the main source of the strengthening mechanism.
4. The additions of Ag and Cu into the Sn-5Sb alloy can increase the solder characteristic, such as the ultimate tensile strength (UTS), and ductility. This is due to the construction of intersmetallic compounds (IMCs) Cu3Sn and Ag3Sn.

5. It is noted that the stress strain parameters, the yield stress, fracture strength, and the total elongation of all alloys are strongly affected by the variation of the strain rate and deformation temperature.

References

1. A.K. Gain, T. Fouzder, Y.C. Chan, A. Sharif, N.B. Wong, W.K.C. Yung, *J. Alloys Compd*., **506**, 216 (2010).
2. R.M. Shalaby, *J. Alloys Compd*. **480**, 334 (2009).
3. A.A. El-Daly, Y. Swilem, A.E. Hammad, *J. Alloys Compd*., **471**, 98 (2009).
4. R. Novakovic, D. Giuranno, E. Ricci, S. Delsante, D. Li, G. Borzone, *Surface Sci*., **605**, 248 (2011).
5. Yu. Plevachuk, W. Hoyer, I. Kaban, M. Köhler, R. Novakovic, *J. Mater. Sci.*, **45**, 2051 (2010).
6. A.A. El-Daly, A.Z. Mohamad, A. Fawzy, A.M. El-Taher, *Mater. Sci. Eng*. A **528**, 1055 (2011).
7. A.K. Gain, T. Fouzder, Y.C. Chan, A. Sharif, W.K.C. Yung, *J. Alloys Compd*. **489**, 678 (2010).
8. A.A. El-Daly, Y. Swilem, M.H.Makled,M.G. El-Shaarawy, A.M. Abdraboh, *J. Alloys Compd*., 484, 134 (2009).
9. M.E. Alam, S.M.L. Nai, M. Gupta, *J. Alloys Compd*., **476**, 199 (2009).
10. Q.S. Zhu, Z.G. Wang, S.D. Wu, J.K. Shang, *Mater. Sci. Eng*. A **502**, 153 (2009).
11. A.R. Geranmayeh, R. Mahmudi, *J. Mater. Sci*., **40**, 3361 (2005).
12. R. Mahmudi, A.R. Geranmayeh, A. Rezaee-Bazzaz, *Mater. Sci. Eng*. A **448**, 287 (2007).
13. K.Kawashima, T. Ito, M. Sakuragi, *Journal of Materials Science*, **27**, 6387 (1992).
14. M.S. Saker, A.Z. Mohamed, A.A. El-Daly, A.M. Abdel-Daiem, A.H. Bassyouni, *Egypt. J. Solids*, **B2**, 34 (1990).
15. A.A. El-Daly, A.E. Hammad, *Mater. Sci. Eng*. A **527**, 5212 (2010).
16. A.A. El-Daly, A.E. Hammad, *J. Alloys Compd*., **505**, 793 (2010).
17. R. Mahmudi, A.R. Geranmayeh, H. Khanbareh, N. Jahangiri, *Mater. Des*. **30**, 574 (2009).